Ivan Vitev

(Transverse) Energy-Energy Correlators at the EIC

Credit for this work goes to my collaborators
H.Li, I.V., Y.J. Zhu, JHEP11 (2020) 051,
H.Li, Y. Makris, I.V., Phys. Rev. D103 (2021) 094005

TMD Collaboration meeting
June 15-17, 2022, Santa Fe, NM

Outline of the talk

- A word about the EIC
- TEEC at the EIC
- BEEC at the EIC
- Conclusions

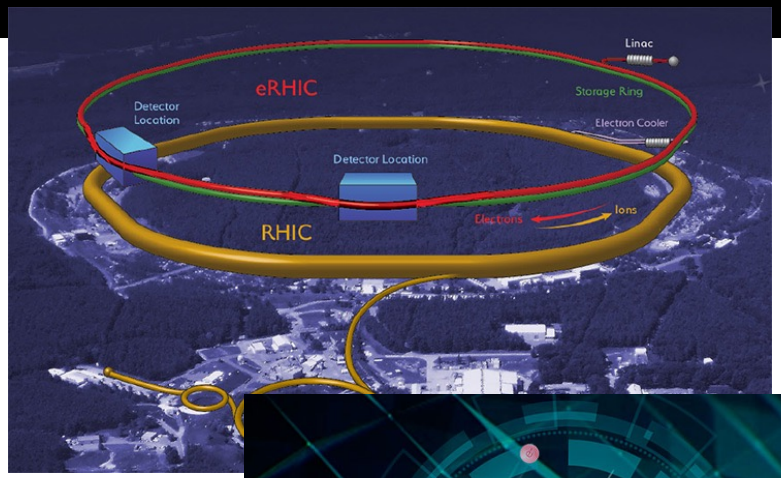

This work is supported by the TMD topical collaboration and the LANL LDRD program

Reference for (T)EEC (prepared for Snowmass)
Reference for references

D. Neill et al. (2022)

TMD Collaboration

LDRD LABORATORY DIRECTED RESEARCH & DEVELOPMENT

Physics

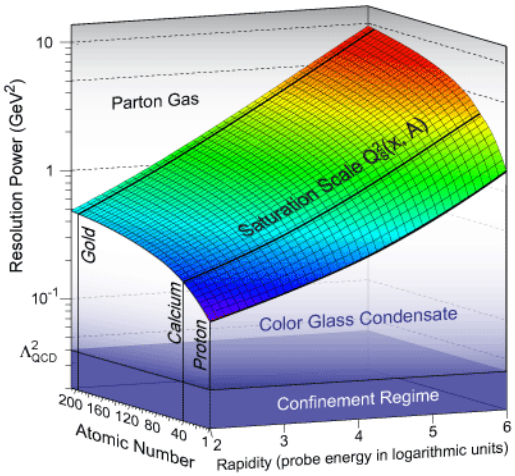

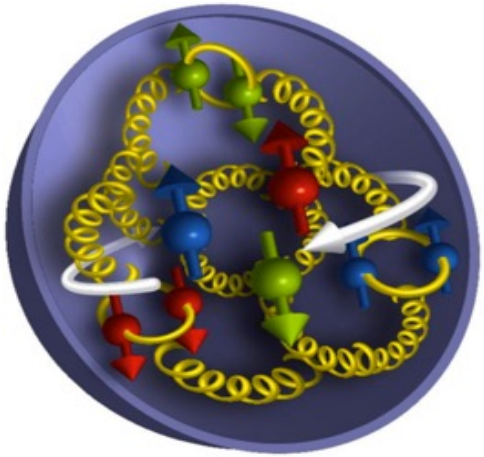

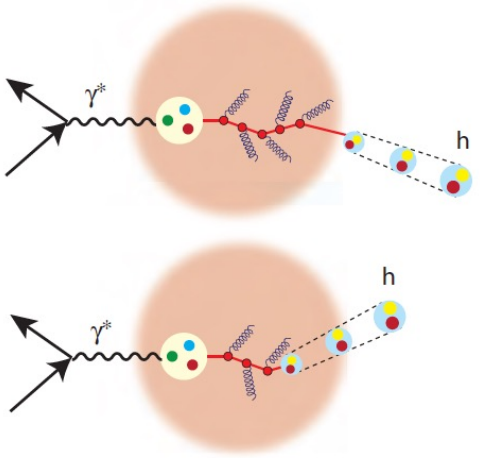

Illustration of EIC focus areas

C. Aidala et al. (2020)

- The origin of mass and the role of gluons
- The internal landscape of nucleons and nuclei, 3D tomography
- The phenomenon of gluon saturation
- Transport properties of large nuclei and the physics of hadronization

A lot of new developments are in the area of jets and heavy flavor

This talk – about the structure of nucleons, precision QCD, TMD physics

I. Transverse Energy-Energy Correlations

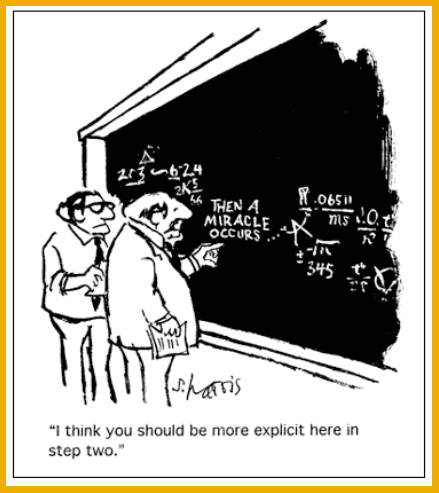

"I think you should be more explicit here in step two."

TMD physics

Introduction to TEEC

electron-positron collider: Basham et al. (1978)

hadronic collider: Ali et al. (1984)

e^+e^- Collisions

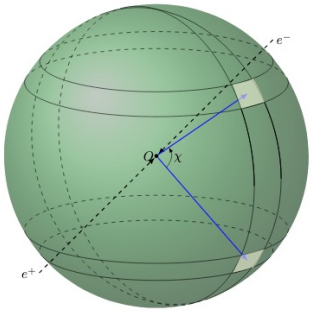

Hadronic initial state

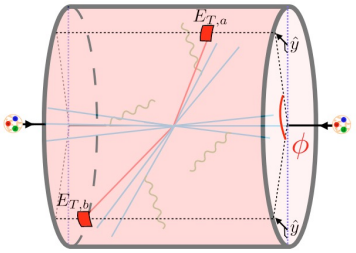

observable

$$\mathrm{EEC} = \sum_{a,b} \int d\sigma_{V\to a+b+X} \frac{2E_aE_b}{Q^2\sigma_{\mathrm{tot}}} \delta(\cos(\theta_{ab}) - \cos(\chi))$$

$$\mathrm{TEEC} = \sum_{a,b} \int d\sigma_{pp\to a+b+X} \frac{2E_{T,a}E_{T,b}}{|\sum_i E_{T,i}|^2} \delta(\cos\phi_{ab} - \cos\phi)$$

- sum over all the jets for each event
- sum over all the particles for each event

Detector lack hermiticity of ones in e+ e- collisions

- Event shape variables can be used to determine the strong coupling αs and test asymptotic freedom, to tune the nonperturbative Quantum Chromodynamics (QCD) power corrections, and to search for new physics phenomena

Successive levels of precision (NLO – N3LO and NLL – N3LL). E.g. in e+e- N3LO and N3LL'

Ebert et al. (2020)

TEEC in the dijet limit and in DIS

$\cos\phi_{ab} \to 0$

Collinear singularity

$J \otimes H$

$\phi \sim 0$

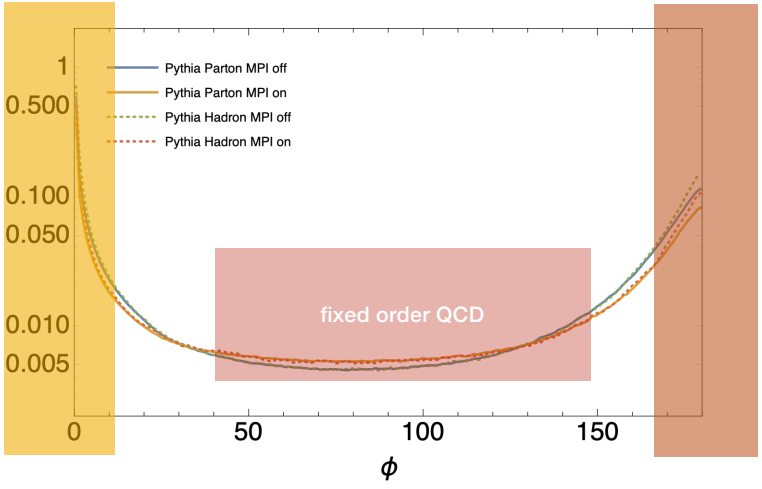

Collinear and soft singularity

$\cos\phi_{ab} \to -1$

$B \otimes H \otimes J \otimes S$

$\phi \sim \pi$

Gao et al. (2018)

Defined as the correlations between the lepton and hadrons in the final state

$$\text{TEEC} = \sum_a \int d\sigma_{lp\to l+a+X} \frac{E_{T,l}E_{T,a}}{E_{T,l}\sum_i E_{T,i}} \delta\left(\cos\phi_{la} - \cos\phi\right)$$

$$\text{TEEC} = \sum_a \int d\sigma_{lp\to l+a+X} \frac{E_{T,a}}{\sum_i E_{T,i}} \delta\left(\cos\phi_{la} - \cos\phi\right)$$

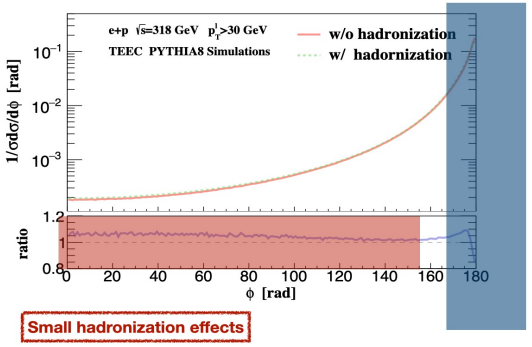

Small hadronization effects

Soft and Collinear radiations dominate

Hadronization effects is less than 20%

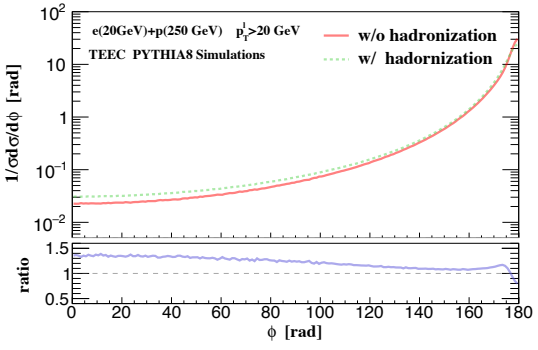

hadronization effects at EIC energy

- ☑ Easier to be measured in DIS
- ☑ NO Collinear singularity when $\phi \to 0$
- ☑ Hadronization effects are suppressed

- Hadronization effects small at HERA but may be non-negligible at EIC

Simulation of TEEC in EIC

$e(18GeV) + p(275GeV)$ Select events with $p_{T,l} > 20GeV$, $-1 < \eta_h < 3$

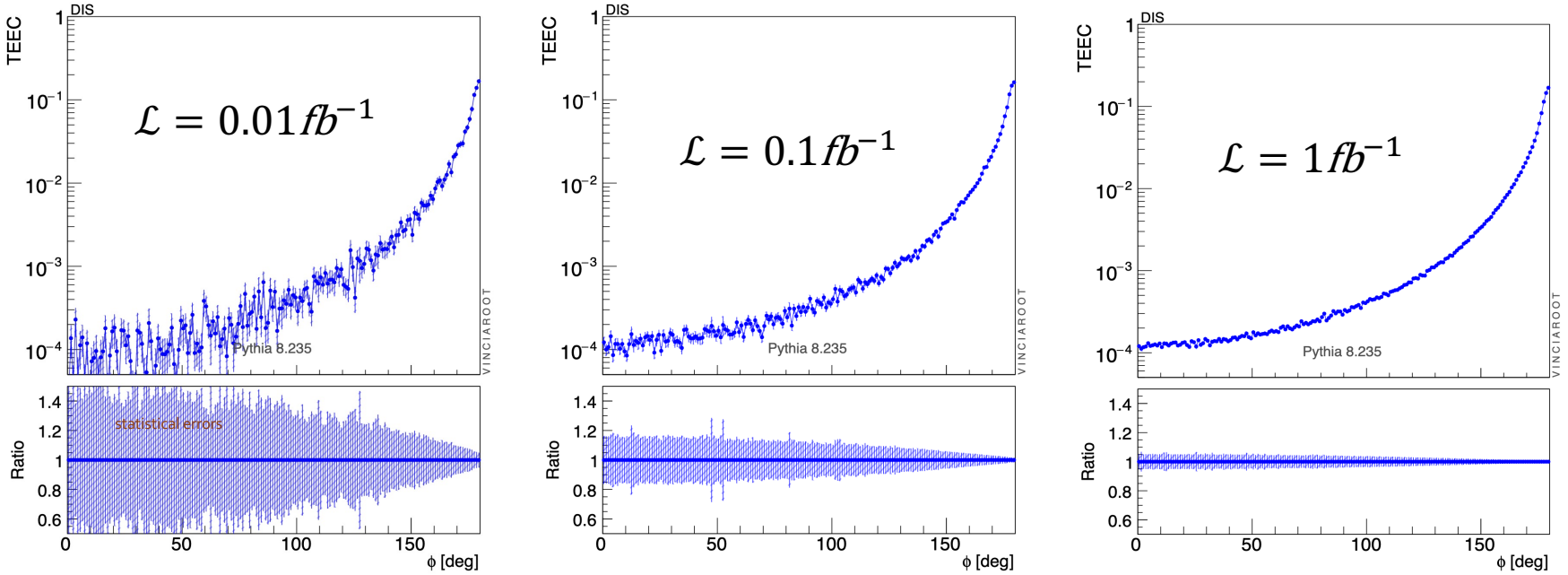

The precision with $10 fb^{-1}$ and $100 fb^{-1}$ will be unprecedented

It does not depend on uncertainties related to the jet radius and jet finding algorithm

TEEC utility: It is possible to study this observable in percent level

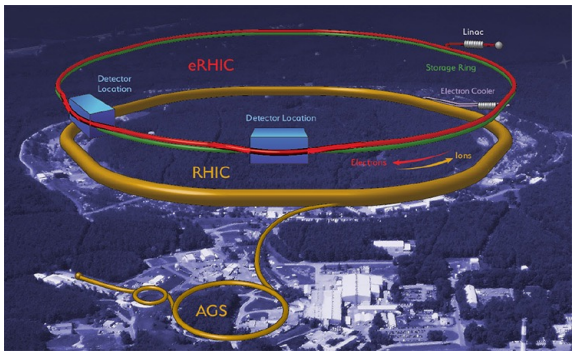

Kinematics and connection to hadron production

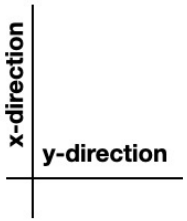

Define scattering plane: x-z

To LO y=o

$$\mathrm{TEEC} = \sum_a \int d\sigma_{lp\to l+a+X} \frac{E_{T,a}}{P_{T,l}} \delta\left(\cos\phi_{la} - \cos\phi\right)$$

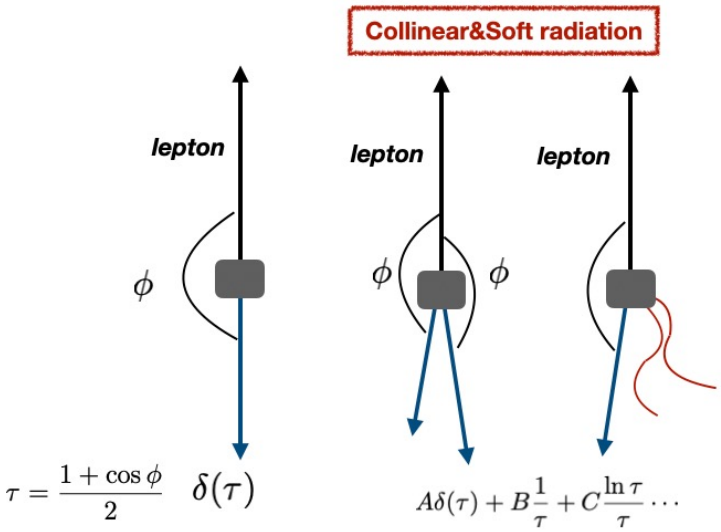

$$\tau = \frac{\left| k_{2,y} - k_{s,y} + \frac{k_{4,y}}{\xi_4} \right|^2}{4p_T^2}$$

For Hadron production

TMD PDF

$$\frac{d\sigma_h}{d^2p_\perp} = \sum_f \int \frac{d\xi dQ^2}{\xi Q^2} Q_f^2 H(Q,\mu) \int \frac{db}{2\pi} e^{ib_\perp \cdot p_\perp} f_{f/N}\left(b,\xi,\mu,\nu\right) S\left(b,\frac{n_2\cdot n_4}{2},\mu,\nu\right) \int \frac{dz}{z^2} F_{h/f}\left(z,b/z,E_4,\mu,\nu\right)$$

TMD soft

TMDFF

For TEEC

- ☑ **Transverse energy weighted**
- ☑ **Measuring vector sum in 1-dimensional**
- ☑ **sum over all hadrons in the final state**

$$\frac{d\sigma_h}{d\tau} = \sum_f \int \frac{d\xi dQ^2}{\xi Q^2} Q_f^2 H(Q,\mu) \int dk_y \int \frac{db}{2\pi} e^{-ib_y\cdot k_y} f_{f/N}\left(b,\xi,\mu,\nu\right) S\left(b,\frac{n_2\cdot n_4}{2},\mu,\nu\right) \sum_h \int z dz\, F_{h/f}\left(z,b/z,E_4,\mu,\nu\right) \delta(\tau - \tau(k_y))$$

Y component generated by soft and collinear radiation

Factorization ingredients

Effectively $(b_x, b_y) \to (0, b_y)$ TMD PDFs can be used

$$S_{\rm DIS}(b) \equiv \frac{1}{N_c}\,{\rm Tr}\left\langle 0 \left| \bar{T}\left[Y_{n_2}(0)Y_{n_4}^{\dagger}(0)\right]^{\dagger} T\left[Y_{n_2}(0)Y_{n_4}^{\dagger}(0)\right] \right| 0 \right\rangle$$

$$Y_{n_2}(x) = \mathcal{P}\exp\left(ig_s\int_{-\infty}^{0} dsn_2\cdot A_s(x+sn_2)\right)$$

$$Y_{n_4}^{\dagger}(x) = \mathcal{P}\exp\left(ig_s\int_{0}^{\infty} dsn_4\cdot A_s(x+sn_4)\right)$$

TEEC soft function $S\left(b, \frac{n_2\cdot n_4}{2}, \mu, \nu\right) = S_{\rm TMD}\left(L_b, L_\nu + \ln\frac{n_2\cdot n_4}{2}\right)$ **TMD soft function**

Jet function

FFs

Matching Coefficients

$$\sum_N \int_0^1 dz z F_{N/q}(z, b_\perp/z, \nu) = \sum_{i,N}\int_0^1 dz z \int_z^1 \frac{d\xi}{\xi}\, d_{N/i}(z/\xi)\, \mathscr{C}_{iq}(\xi, b_\perp/\xi, \nu) + \mathcal{O}\left(b_T^2\Lambda_{\rm QCD}^2\right) = \sum_{i,N}\int_0^1 dx x \mathscr{C}_{iq}(x, b_\perp/\xi, \nu)\int_0^1 d\xi\xi d_{N/i}(\xi) + \mathcal{O}\left(b_T^2\Lambda_{\rm QCD}^2\right)$$

Momentum conversvation

$${\rm TEEC} = \sum_a \int d\sigma_{lp\to l+a+X}\frac{E_{T,a}}{\sum_i E_{T,i}}\delta(\cos\phi_{la} - \cos\phi)$$

The jet function is the second Mellin-moment of the matching coefficients

$$J^q(b_\perp, \mu, \nu) = \sum_i \int_0^1 dx x \mathscr{C}_{iq}(x, b_\perp/x, \mu, \nu)$$

- Ways in which TMD physics enters the calculation

Factorization in the back-to-back limit

$$ep \to e + \text{jet} \qquad \frac{d\sigma^{(0)}}{d\tau} = \sum_f \int \frac{d\xi dQ^2}{\xi Q^2} Q_f^2 \sigma_0 \int \frac{db}{2\pi} e^{-2ib\sqrt{\tau} p_T} H(p_T, Q, \mu) S(b, Q, \mu, \nu) B_{f/N}(b, \xi, \mu, \nu) J_f(b, \mu, \nu)$$

$$\sum_{i=1} \alpha_s^i L^{2i} + \sum_{i=1} \alpha_s^i L^{2i-1} + \sum_{i=1} \alpha_s^i L^{2i-2} + \sum_{i=2} \alpha_s^i L^{2i-3} + \sum_{i=2} \alpha_s^i L^{2i-4} + \sum_{i=3} \alpha_s^i L^{2i-5}$$

NLL NNLL NNNLL

Fixed order in back-to-back limit

The leading order process is

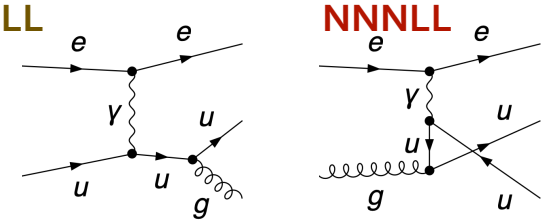

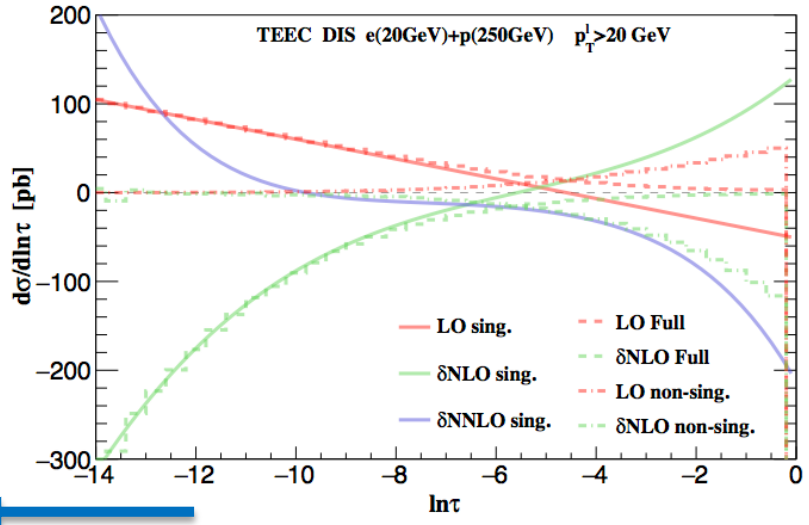

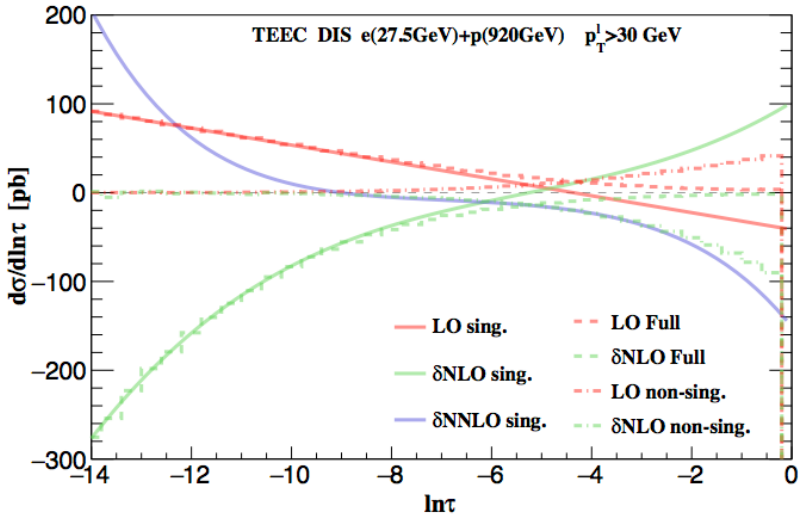

Back-to-back

Full control of the distributions in the back-back limit

A word about evolution

Factorization scale

Hard

$$\frac{d}{d\ln\mu}\ln H(Q^2,\mu) \equiv \Gamma_h = 2C_F\gamma_{\rm cusp}\ln\frac{Q^2}{\mu^2} + 2\gamma_q$$

Beam, Jet

$$\frac{d}{d\ln\mu}\ln \mathcal{G}_i = -C_F\gamma_{\rm cusp}\ln\frac{4E_i^2}{\nu^2} + \gamma_{G,i}$$

Soft

$$\frac{d}{d\ln\mu}\ln S \equiv \Gamma_s = -2C_F\gamma_{\rm cusp}\ln\frac{\nu^2 n_2\cdot n_4}{2\mu^2} - 2\gamma_s$$

- X-section Scale invariance

$$2\gamma_q + \gamma_{B,q} + \gamma_{J,q} - 2\gamma_s = 0$$

$$2\ln\frac{Q^2}{\mu^2} - \ln\frac{4E_2^2}{\nu^2} - \ln\frac{4E_4^2}{\nu^2} - 2\ln\frac{\nu^2 n_2\cdot n_4}{2\mu^2} = 0$$

$$Q^2 = 4E_2E_4\frac{n_2\cdot n_4}{2}$$

Rapidity scale

Hard -

Beam, Jet

$$\frac{d}{d\ln\nu}\ln\mathcal{G}_i = C_F\left[\int_{b_0^2/b^2}^{\mu^2}\frac{d\bar{\mu}^2}{\bar{\mu}^2}\gamma_{\rm cusp}(\bar{\mu}) - \gamma_r(b_0^2/b^2)\right]$$

Soft

$$\frac{d}{d\ln\nu}\ln S = 2C_F\left[-\int_{b_0^2/b^2}^{\mu^2}\frac{d\bar{\mu}^2}{\bar{\mu}^2}\gamma_{\rm cusp}(\bar{\mu}) + \gamma_r(b_0^2/b^2)\right]$$

- X-section Scale invariance

$$\frac{d}{d\ln\nu}\ln B_q + \frac{d}{d\ln\nu}\ln J_q + \frac{d}{d\ln\nu}\ln S = 0$$

Exponential rapidity regulator

Resummation in the back-to-back limit

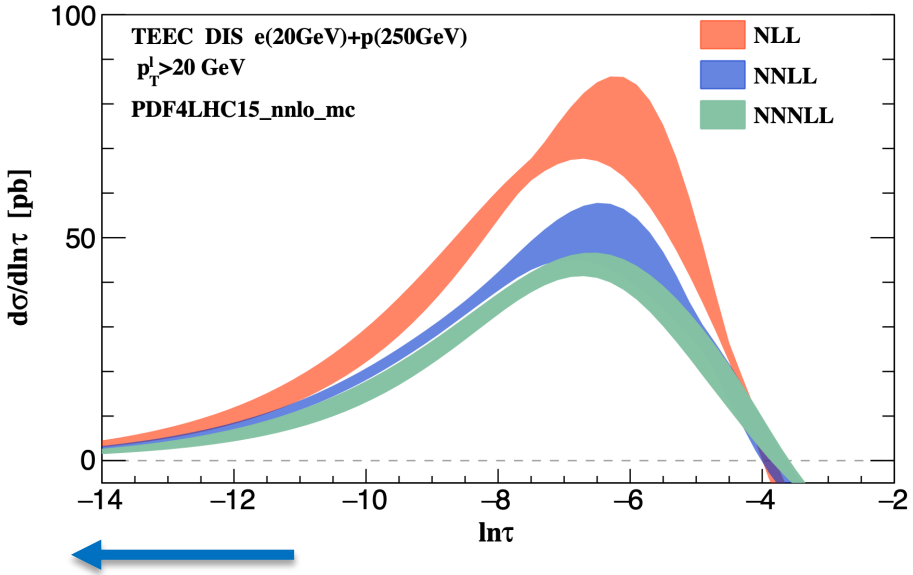

Back-to-back

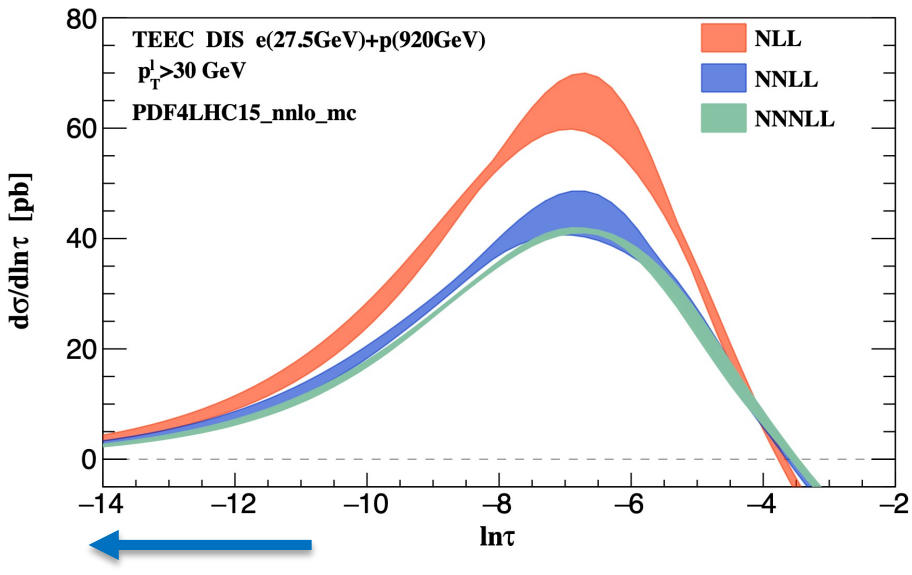

Back-to-back

- Convergence in back-to-back limit after resummation
- Resummation works better for higher energy collider due to larger scale hierarchy
- Huge difference from NLL to NNLL and good perturbative convergence from NNLL to NNNLL
- Reduction of scale uncertainties order by order from NLL to NNNLL

The highest resummed accuracy in DIS at the time

Note that an absolute cross section is shown, not normalized. Thus there is overall value change order-by-order.

Final results and NP corrections

$$S_{\mathrm{NP}} = \exp[-0.106b^2 - 0.84\ln Q/Q_0 \ln b/b^*]$$

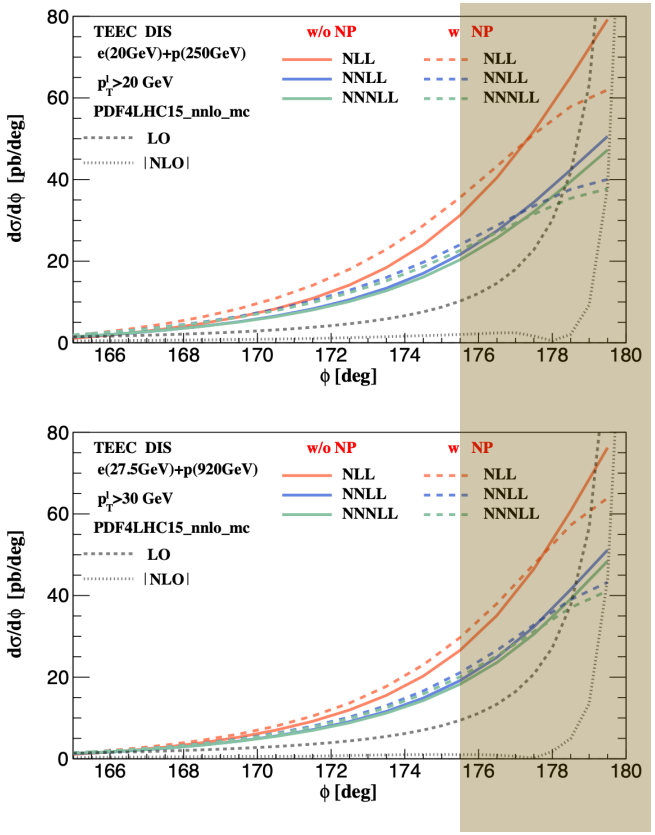

Finite after resummation

Relative large NP effects

Nuclear matter effects are expected in this region

NP shifts the cross section

Expect: NNLO matching will improve the predictions

$$\frac{d\sigma_{\mathrm{N^lLL+N^kLO}}}{d\tau} = \frac{d\sigma_{\mathrm{N^lLL}}}{d\tau} + \frac{d\sigma_{\mathrm{N^kLO}}}{d\tau} - \left(\frac{d\sigma_{\mathrm{N^kLO}}}{d\tau}\right)_{\mathrm{sing.}}$$

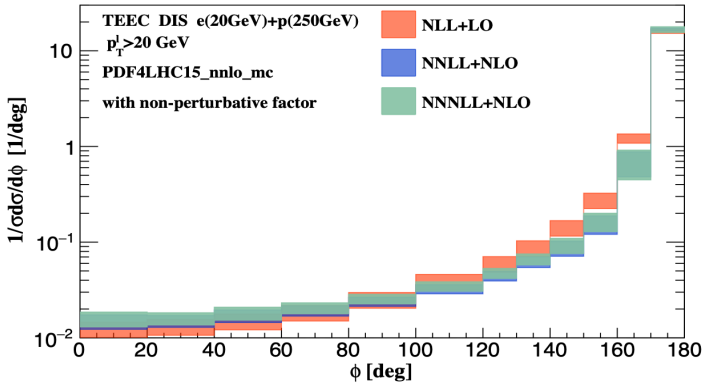

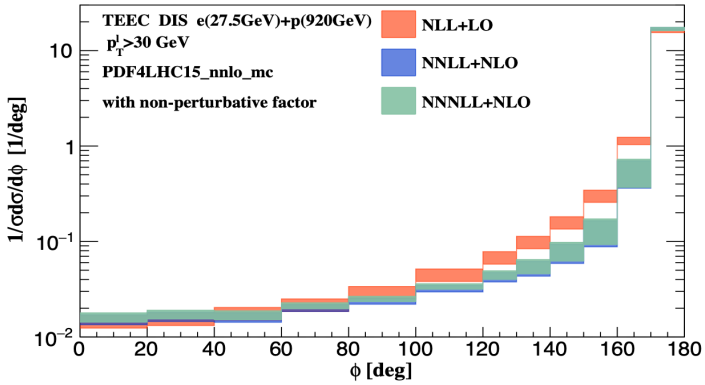

Uncertainties from fixed order are dominant

Prediction in full ϕ range

Matching was done numerically

NNLO event shapes

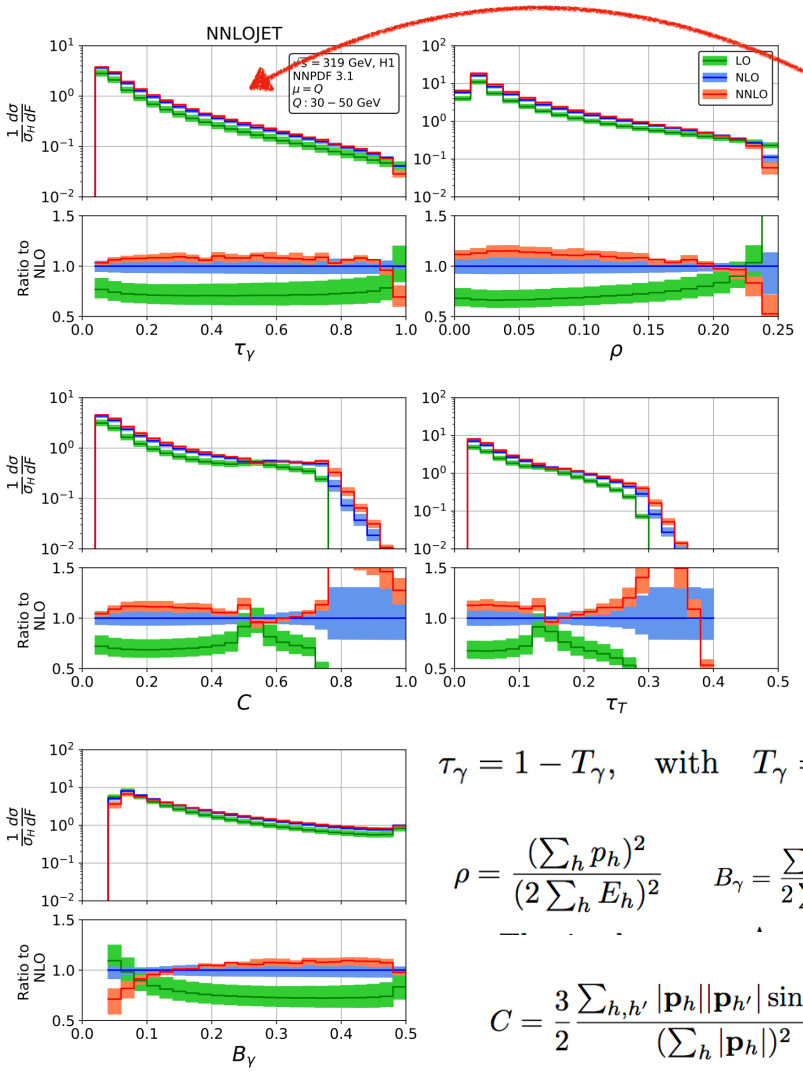

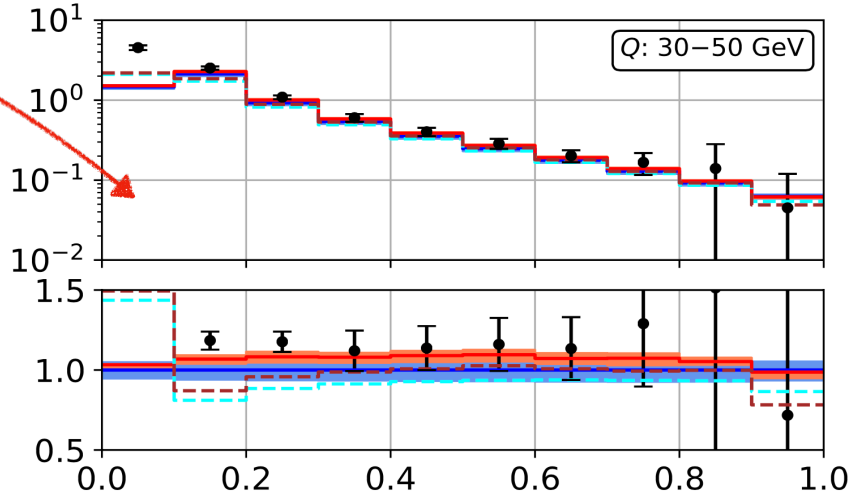

with non-perturbative corrections

$$\tau_\gamma = 1 - T_\gamma, \quad \text{with} \quad T_\gamma = \frac{\sum_h |p_{z,h}|}{\sum_h |\mathbf{p}_h|}$$

$$\rho = \frac{(\sum_h p_h)^2}{(2\sum_h E_h)^2} \qquad B_\gamma = \frac{\sum_h |\mathbf{p}_{t,h}|}{2\sum_h |\mathbf{p}_h|}$$

$$C = \frac{3}{2}\frac{\sum_{h,h'} |\mathbf{p}_h||\mathbf{p}_{h'}| \sin^2\theta_{hh'}}{(\sum_h |\mathbf{p}_h|)^2}$$

- It is not always to be true that NLO will improve the theoretical uncertainties
- NNLO corrections reduce the uncertainties
- Large nonperturbative corrections for most of event shape variables

Gehrmann, Huss, Mo, Niehues, 2019

II. Energy Energy Correlations in the Breit frame

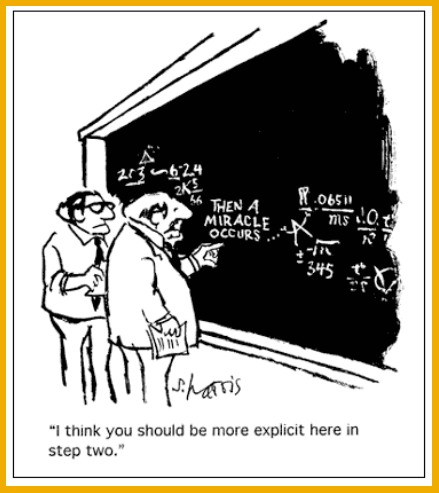

"I think you should be more explicit here in step two."

TMD physics

The Breit frame

Traditionally used in DIS

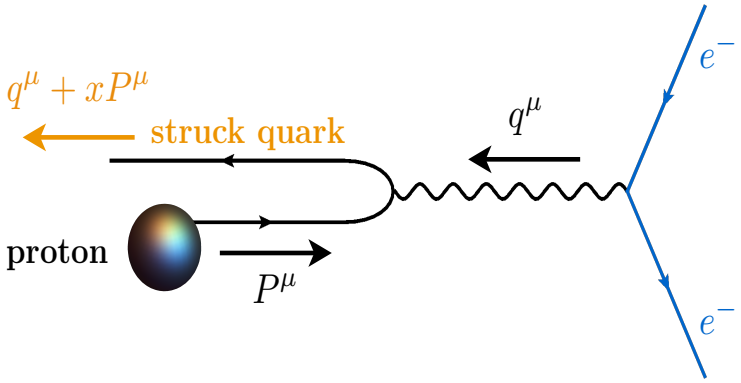

$$q^\mu = \frac{Q}{2}(\bar{n}^\mu - n^\mu) = Q(0,0,0,-1)$$

$$p_q^\mu = xP^\mu + q^\mu \simeq (Q/2)\bar{n}^\mu$$

$$P^\mu \simeq Q/(2x_B)n^\mu = Q/(2x_B)(1,0,0,+1)$$

$$z_a = \frac{P \cdot p_a}{P \cdot q} \xrightarrow[\text{frame}]{\text{Breit}} z_a = n \cdot p_a/Q = p_a^+/Q$$

$$\sum_a z_a = 1$$

- Invariant energy fraction taken by the particle
- Sum over all particles form the struck quark, no scattered lepton included

Goal: ``Backward-EEC" (or BEEC) to emphasize that this is a new definition which focuses to the contribution of the back-scattered struck quark direction. Separates beam remnants, soft radiation, and the above struck quark fragmentation. Definition spherically invariant

BEEC Definition, EFT modes, factorization

$$\text{BEEC} = \frac{1}{\sigma}\sum_a \int d\sigma(\ell + h \to \ell + a + X)\; z_a\; \delta(\cos\theta_{ap} - \cos\theta)$$

θ_{ap} **Opening angle between the direction of the particle and the direction of the proton**

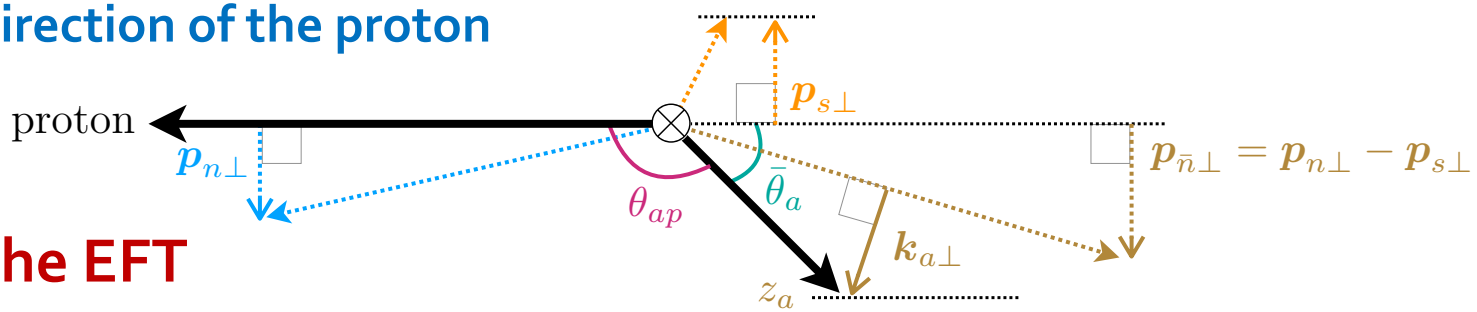

Modes in the EFT

$$n\text{-collinear}: \quad p_n^\mu \sim Q(\lambda^2, 1, \lambda)$$

$$\bar{n}\text{-collinear}: \quad p_{\bar{n}}^\mu \sim Q(1, \lambda^2, \lambda)$$

$$\text{soft}: \quad p_s^\mu \sim Q(\lambda, \lambda, \lambda)$$

- Expanding around the quark direction one sees the relation to TMD physics

$$\frac{\pi - \theta_{ap}}{2} = \frac{\bar{\theta}_a}{2} \simeq \frac{|\boldsymbol{q}_\perp|}{Q} \simeq \frac{1}{Q}\left|\frac{\boldsymbol{k}_{a\perp}}{z_a} + \boldsymbol{p}_{n\perp} - \boldsymbol{p}_{s\perp}\right|$$

$$\frac{d\sigma_a}{dx dQ^2 dz d\tau} = \int d\boldsymbol{q}_\perp \frac{d\sigma_a}{dx dQ^2 dz d\boldsymbol{q}_\perp}\delta\left(\tau - \frac{|\boldsymbol{q}_\perp|^2}{Q^2}\right)$$

$$\frac{d\sigma_a}{dx dQ^2 dz d\boldsymbol{q}_\perp} = \sigma_0(Q, x, y) H_{ij}(Q, x; \mu) \int \frac{d\boldsymbol{b}}{(2\pi)^2} \exp(-i\,\boldsymbol{b}\cdot\boldsymbol{q}_\perp) B_{j/P}(x, b; \mu, \nu) D_{i/a}(z, b; \mu, \nu) S(b; \mu, \nu)$$

TMD factorization

Numerical results – FO calculations and resummation

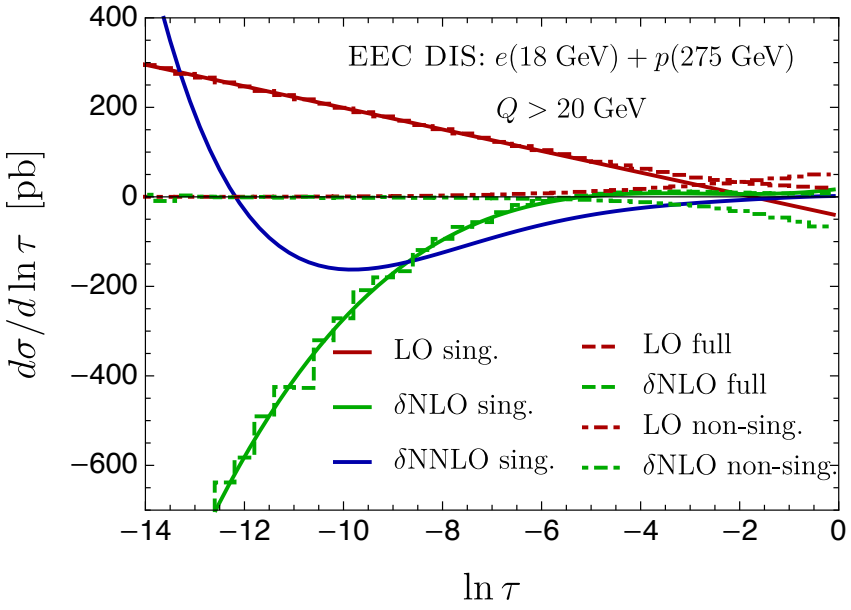

Fixed order full QCD cone with NLOJET++

Fixed-order ln(tau) distributions in z -> 1 limit. The solid lines represent the singular distribution prediction by SCET. The dashed lines are the fixed order QCD results. The dash-dotted lines are power corrections.

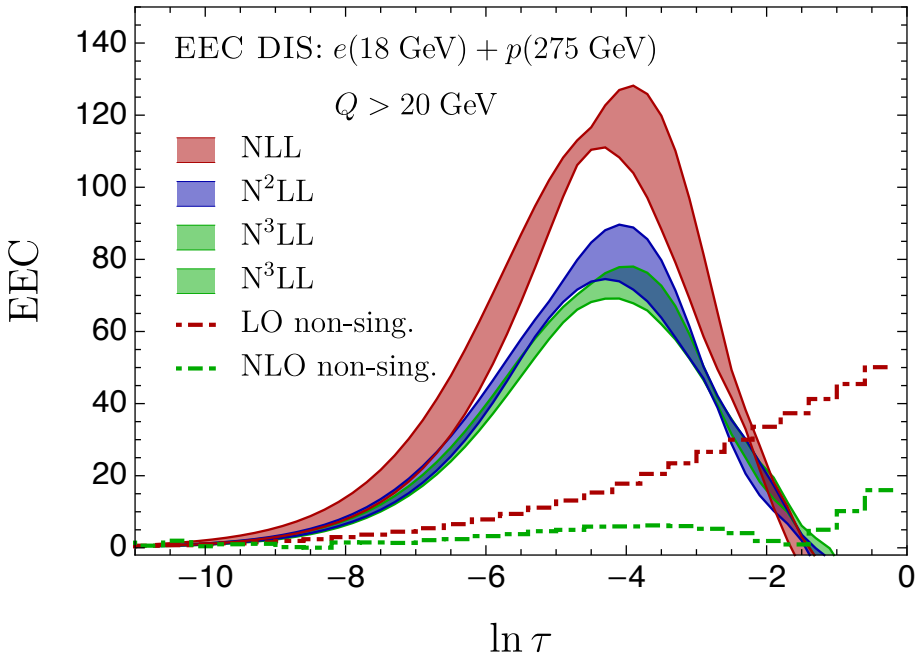

Resummed ln(tau) $ distributions for EEC. The dark red, dark blue, and dark green bands correspond NLL, NNLL, and NNNLL distribution. The dot-dashed lines are the LO non-singular distributions (dark red) and the absolute value of NLO non-singular ones (dark green)

Numerical results – non-perturbative effects, comparison

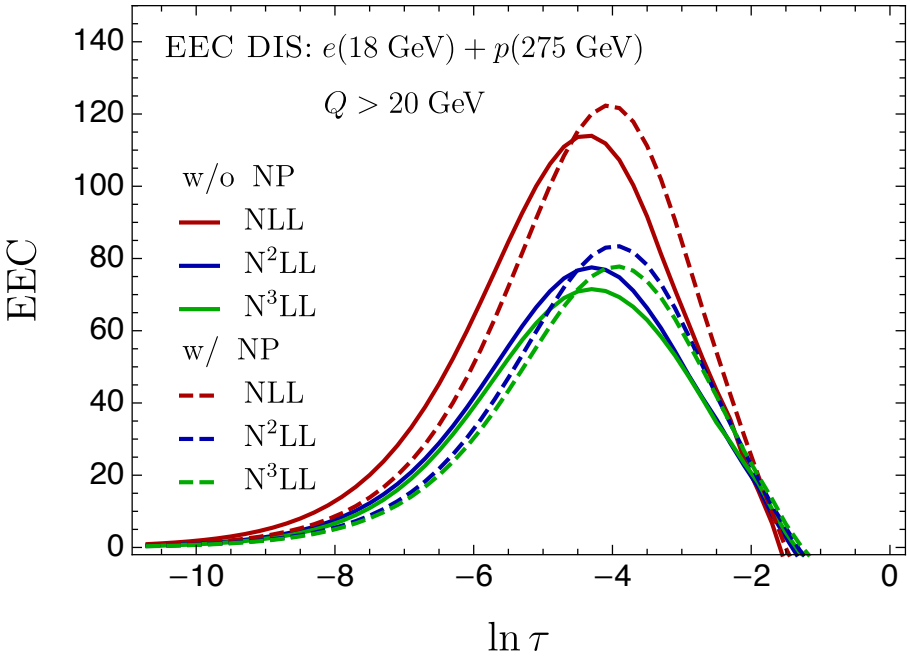

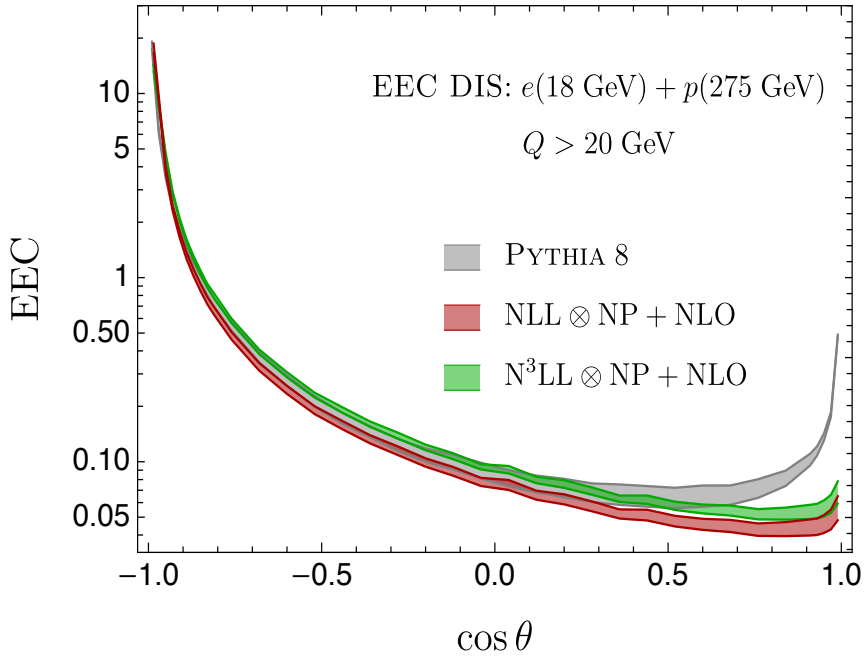

Resummed ln(tau) distributions without (solid) and with non-perturbative factor.

$$f_{\rm NP} = \exp\Big(-0.106\ b^2 - 0.84 \ln Q/Q_0 \ln b/b^* \Big)$$

Non-perturbative factor

Comparison of cos(theta) distributions between the SCET Predictions and PYTHIA simulations. The dark red and dark green bands are the NLL+NLO and N3LL+NLO. The gray band are from PYTHIA 8 simulations with the default settings for uncertainty bands.

Advantages of BEEC – reduced rapidity cuts sensitivity

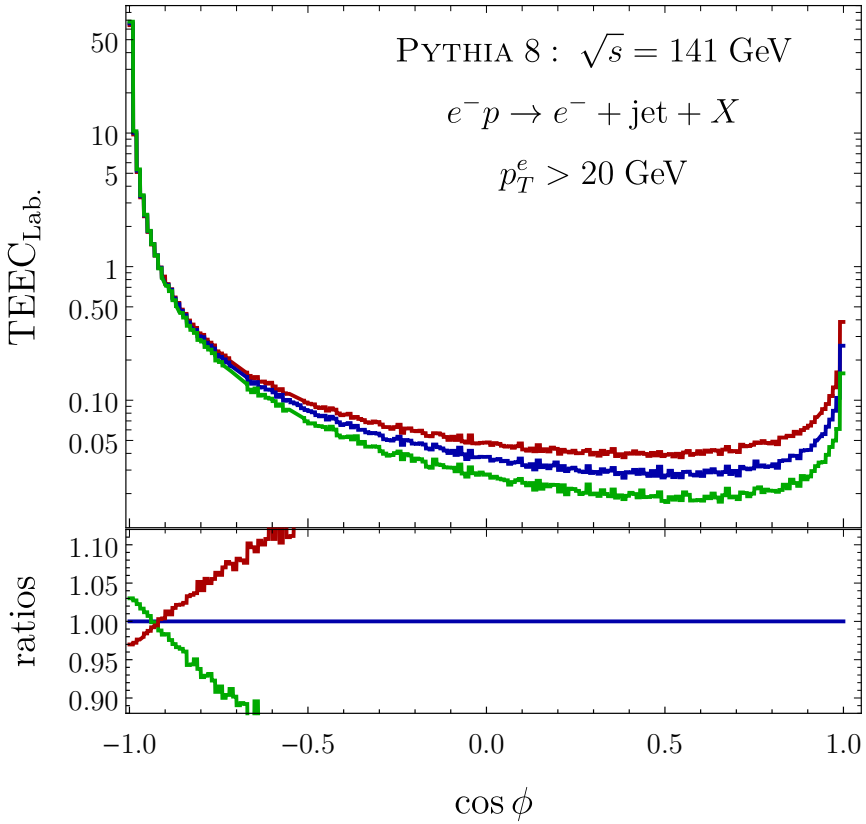

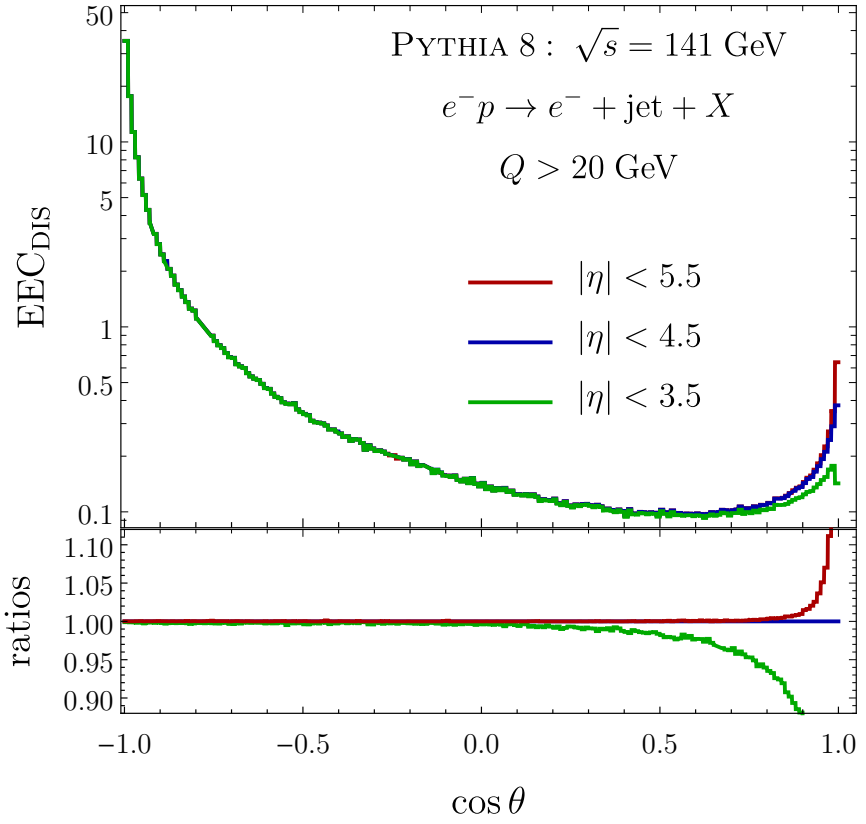

For TEEC the distribution can vary by more than a factor of 2 at intermediate angle depending on the rapidity cuts. For BEEC this sensitivity is eliminated except for small angles (on the beam direction)

Conclusions

- We introduced transverse energy-energy correlators TEEC to DIS - promising way to study TMD physics and non-perturbative effects
- We performed the most accurate at the time NLO+NNNLL calculation for the EIC. Uncertainties dominated by the FO calculation
- We are also introduced/studied backward energy-energy correlators in the Breit frame BEEC – to further elucidate the connection to TMD physics. Better separation of physics contributions and less sensitive to rapidity cuts
- In the future one can improve the calculation by matching to NNLO fixed order, explore other models of non-perturbative effects
- The (T)EEC can be measured with high accuracy in DIS.